Effects of Contact-Stress on Hot-Embossed PMMA Microchannel Wall Profile

Kin Fong Lei [1,2], Wen J. Li [1,2,*], and Yeung Yam[2]

[1] *Centre for Micro and Nano Systems,*

[2] *Department of Automation and Computer-Aided Engineering,*

The Chinese University of Hong Kong, Shatin, Hong Kong SAR.

[*] Tel: +852 26098475 Fax: +852 26036002 E-mail: wen@acae.cuhk.edu.hk

ABSTRACT

Hot-embossing (thermal-compression) based microchannel fabrication techniques have gained much attention recently due to their low-cost setup and ease of implementation. However, not much has been done in trying to understand or characterize the mechanics of the hot-embossing process in fabricating microchannels. Hence, most research groups still rely on trial-and-error processes to hot-emboss microchannels for microfluidic control applications. Our ongoing effort is to develop a quantitative method to understand the hot-embossing mechanism of using molds with micro-features to hot-emboss PMMA substrates. Our experimental results proved that the *contact-stress* analysis is a very good approach to model hot-embossing of microchannels on polymer substrates because the resulting channel wall profile can be predicted with good accuracy using a close-form solution. In this paper, the formulation of contact-stress analysis and our experimental validation of microchannels are also described.

1. INTRODUCTION

Although materials such as silicon and glass are excellent choices for electronic and mechanical devices, they may not be the first choice for applications in biology and chemistry that require fluidic devices. Since fluidic devices require more surface area than electronic circuits and their interface with the external world is more complicated, the most commonly used

micromachining methods (e.g., silicon etching) and materials (e.g., single crystalline silicon) are relative expensive for fluidic devices. For example, a micropump usually has a larger chip size (in the order of $1cm^2$) and consists of three or more layers [1]. Hence, for mass fabrication of fluidic devices, silicon micromachining is not the only possible cost effective fabrication method.

Hot-embossing (thermal-compression) based micro-fluidic device fabrication technique has gained much attention recently due to its low-cost setup and ease of implementation. It is a flexible and low-cost microfabrication method for high aspect ratio polymer based microstructures. By using the electroplated metal mold to "imprint" micro features on polymer substrates, many fully patterned substrates can be produced in a short production cycling time. Many microfluidic devices have already been fabricated by using the hot-embossing technique (e.g., [2, 3]). The various available processes are capable of producing polymer-based channels with widths ranging from a few hundred microns (using SU-8 based electroplated molds) to a few hundred nanometers (using CD based molds) as we have demonstrated recently [4, 5]. However, to the best of our knowledge, not much has been done in trying to understand or characterize the mechanics of the hot-embossing process in fabricating microstructures. Hence, most research groups still rely on trial-and-error processes to hot-emboss microstructures for microfluidic control applications. Our ongoing effort is to develop a quantitative method to understand the hot-embossing mechanism of using molds with micro-features to hot-emboss polymethylmethacrylate (PMMA) substrates. Our experimental results proved that the *contact-stress* analysis is a very good approach to model hot-embossing of microchannels on polymer substrates because the resulting channel wall profile can be predicted with good accuracy using a close-form solution. The formulation of this analysis and our experimental validation are described in this paper.

2. PMMA MECHANICAL ANALYSIS

PMMA is a hard, rigid and transparent material at room temperature. But, by varying the temperature, its mechanical, electrical and other properties will be changed significantly. Normally, molecules may occur in three states: solid, liquid and gaseous state. The transitions between these states are sharp. In the case of polymer molecules, the situation is much more complex. In solid state, polymer is only exceptionally purely crystalline, but generally it is partially or totally amorphous. A specific amorphous polymer, such as PMMA, can exist in a number of states according to its temperature [6]. A clearly defined melting point of PMMA no longer occurs and a rubbery intermediate zone is often observed. In this case, two transition temperatures may be observed: firstly a rigid solid-rubber transition (usually known as the glass transition temperature, T_g) and secondly a generally very indefinite rubber-liquid transition. In solid state, PMMA is hard, rigid and transparent. Thus, the material is glass-like so that sometimes it referred to as the glassy state. At this state, molecular movements other than bond vibrations are very limited. However, above the glass transition temperature, the molecule has more energy, and movement of molecular segments becomes possible. The molecules naturally take up a random and coiled conformation as a result of free rotation about single covalent bond in the chain backbone. If a specimen is heated to a temperature above its glass transition point and then subjected to a tensile stress, the molecules will tend to align themselves in the general direction of the stress. If the mass is then cooled below its transition temperature while the molecule is still under stress, the molecules will become frozen whilst in an oriented state.

Based on the above properties of PMMA, it is possible to explain the physical phenomenon that occurs when the hot-embossing process is applied on PMMA substrate, i.e., localized deformation and re-solidification of the substrate. However, this does not give a quantitative explaination on the geometry of the localized deformation after the heat-compression process. To derive the mechanical model of a heated mold compressed onto a heated PMMA substrate, Hooke's

law for stress-strain relationship can be used to model the cross sectional displacement profile of the substrate surface. As will be discussed in the next section, this stress-strain relationship depends on the Young's modulus, which varies with temperature, the Poisson ratio (assumed to be independent of temperature, ν=0.4), the channel mold feature width, the temperature of the PMMA, and the pressure applied onto the PMMA from the mold. To determine the temperature dependence of Young's modulus for the PMMA used in our molding process (2.0mm thick Cast Acrylic, RS Component), a Hounsfield tensile tester was used to collect the stress-strain data and a Minolta spot thermometer was used to measure the surface temperature of the PMMA specimen. The load-displacement relationship for a typical PMMA specimen at various temperatures is shown in Figure 1. From the figure, we observed that the PMMA is in glassy state when temperature is below 102°C, rubbery state when temperature is above this temperature. We can conclude that this PMMA specimen has the glass transition temperature at 102°C. From those experimental data, we can calculate the Young's modulus as a forth order polynomial function of temperature, as shown in Figure 2 and equation (1):

$$\log E(T) = -1.3909\times10^{-7}T^4 + 6.5716\times10^{-5}T^3 - 0.0107T^2 + 0.6707T - 4.9704 \quad (1)$$

where E is Young modulus (MPa), T is temperature (°C). These experimental parameters allowed us to determine the Young's modulus of our PMMA substrates at different temperatures during the hot-embossing process. This expression is also useful in calculating the strain and displacement field once the stress field is known, as will be presented in the next section.

3. MODELING HOT-EMBOSSING BY CONTACT STRESS ANALYSIS

Although the hot-embossing process is a fast replication process, one of its shortcomings is the difficulty of transferring sharp straight wall features from a mold to a polymer substrate (see Figure 3). This is mainly due to the contact-stress caused by the mold on a substrate. Using contact-stress analysis [7], we were found that it is a very good approach to model the cross sectional profile of microchannels on polymer substrates after the hot-embossing process.

Consider a contact stress p acting over an infinitesimal surface area tdy_1, as shown in Figure 4, at an isolated surface at a distance r, the radial stress is given with the net force $P = ptdy_1$. This stress can be expressed as:

$$\sigma_r = -\frac{2}{\pi r} pdy_1 \cos\theta, \quad \sigma_\theta = 0, \quad \tau_{r\theta} = 0 \tag{2}$$

These stresses must satisfy the boundary condition, that the net force P balances the sum of the resultant forces acting on a cylindrical surface of radius r, or:

$$2\int_0^{\pi/2} \sigma_r \cos\theta \cdot r d\theta = -\frac{4P}{\pi}\int_0^{\pi/2} \cos^2\theta d\theta = -P \tag{3}$$

The stresses with respect to the xy coordinate system are represented by

$$\begin{aligned} \sigma_x &= \sigma_r \cos^2\theta = -\frac{2}{\pi r} pdy_1 \cos^3\theta \\ \sigma_y &= \sigma_r \sin^2\theta = -\frac{2}{\pi r} pdy_1 \sin^2\theta\cos\theta \\ \tau_{xy} &= \sigma_r \sin\theta\cos\theta = -\frac{2}{\pi r} pdy_1 \sin\theta\cos^2\theta \end{aligned} \tag{4}$$

If *xy* are used in place of $r\theta$, equation (2) can be transformed using the relations

$$r = \sqrt{x^2 + y^2}, \quad \cos\theta = \frac{x}{\sqrt{x^2 + y^2}}, \quad \sin\theta = \frac{y}{\sqrt{x^2 + y^2}}$$

Thus

$$\begin{aligned} \sigma_x &= -\frac{2}{\pi} p dy_1 \frac{x^3}{(x^2 + y^2)^2} \\ \sigma_y &= -\frac{2}{\pi} p dy_1 \frac{xy^2}{(x^2 + y^2)^2} \\ \tau_{xy} &= -\frac{2}{\pi} p dy_1 \frac{x^2 y}{(x^2 + y^2)^2} \end{aligned} \tag{5}$$

For a contact stress *p* acting on an area at a distance y_1 away from the origin (as shown in Figure 5), the stresses can be found simply by substituting $y - y_1$ for y in equations (3). Thus

$$\begin{aligned} \sigma_x &= -\frac{2}{\pi} p dy_1 \frac{x^3}{[x^2 + (y - y_1)^2]^2} \\ \sigma_y &= -\frac{2}{\pi} p dy_1 \frac{xy^2}{[x^2 + (y - y_1)^2]^2} \\ \tau_{xy} &= -\frac{2}{\pi} p dy_1 \frac{x^2 y}{[x^2 + (y - y_1)^2]^2} \end{aligned} \tag{6}$$

Consider the hot embossing process, where the contact force from the hydraulic press is uniformly distributed on the polymer substrate, as shown in Figure 6a. The stress distribution from a microchannel mold feature on the substrate is assumed to be a constant pressure distribution $p(y_1)=p_o$ in the region $-a \le y \le a$ as shown in Figure 6b. Integrating y_1 from $-a$ to *a*, stress in the x-direction is

$$\sigma_x = -\frac{2}{\pi} p_o x^3 \int_{-a}^{a} \frac{dy_1}{[x^2 + (y - y_1)^2]^2} \tag{7}$$

Let $u = y - y_1$, thus, $du = -y_1$, and (7) becomes

$$\sigma_x = -\frac{2}{\pi} p_o x^3 \int_{y+a}^{y-a} \frac{du}{(x^2 + u^2)^2} \tag{8}$$

Integrating (8) yields

$$\sigma_x = \frac{2}{\pi} p_o x \left[\frac{u}{2(x^2 + u^2)} + \frac{1}{2x} \tan^{-1} \frac{u}{x} \right]_{y+a}^{y-a} \tag{9}$$

Substituting the limits of integration and simplifying, the stresses can be written as in equation (10).

$$\begin{aligned}
\sigma_x &= \frac{p_o}{\pi} \left\{ \frac{2ax(y^2 - x^2 - a^2)}{[x^2 + (y-a)^2][x^2 + (y+a)^2]} + \tan^{-1}\left(\frac{y-a}{x}\right) - \tan^{-1}\left(\frac{y+a}{x}\right) \right\} \\
\sigma_y &= \frac{p_o}{\pi} \left\{ \frac{2ax(x^2 + a^2 - y^2)}{[x^2 + (y-a)^2][x^2 + (y+a)^2]} + \tan^{-1}\left(\frac{y-a}{x}\right) - \tan^{-1}\left(\frac{y+a}{x}\right) \right\} \\
\tau_{xy} &= -\frac{4p_o}{\pi} \frac{ax^2 y}{[x^2 + (y-a)^2][x^2 + (y+a)^2]}
\end{aligned} \tag{10}$$

For calculating the strains when the stresses are known, when the substrate is in elastic region, Hooke's law can be applied. Note, when the polymer substrate is above glass transition temperature, it becomes rubbery, and does not have a plastic stress-strain region (see Figure 1), so this equation can still be used. Using Hooke's law, strains can be related to the Young's modulus *E*, Poisson ratio ν, and stresses by:

$$\varepsilon_x = \frac{1}{E}(\sigma_x - \nu\sigma_y), \quad \varepsilon_y = \frac{1}{E}(-\nu\sigma_x + \sigma_y) \tag{11}$$

Integrating the strain by substrate thickness, the displacement δ can be calculated. Note that the Young's modulus E is temperature dependent in the above equation.

$$\delta_x = \int \varepsilon_x dx \tag{12}$$

Using the above contact-stress analysis, the deformation of the polymer substrate surface after the hot-embossing process can be modeled. In next section, the comparison of numerical modeling using the contact-stress analysis and experimental data is presented.

4. EXPERIMENTAL VALIDATION

By the contact-stress analysis discussed in the last section, 2D stress field on a polymer substrate due to a uniform contact pressure field p_o applied over an infinitesimal surface area $2a$ can be calculated by using equation (10). In the hot-embossing process, a PMMA substrate is heated above its glass transition temperature and embossed by a metal mold with micro-features. During this process, PMMA substrate is in elastic region (see Figure 1 for $T > 102°C$) and under a uniform distributed contact pressure. Contact-stress analysis can be applied reasonably.

A PMMA substrate was embossed at 120°C to obtain microchannels of different widths, as shown in Figure 7. We found that it is difficult to transfer sharp straight wall features to the PMMA substrate. From the description of contact-stress analysis, the deformation of the PMMA depends on the applied pressure and temperature. Hence, we conducted various experiments to compare the microchannel cross sectional profiles between the numerical results of the contact-stress analysis and experimental data. The microchannel profiles were measured by an Alpha-step profiler in the following comparisons.

4.1. Different pressures, same temperature and channel width.

PMMA substrates were embossed at 120°C under different pressures, and the channel width is 1000μm. The comparison of the modeled results (numerical solution of contact-stress analysis) and experimental data is plotted in Figure 8. From the numerical results, we estimated the pressures were 19×10^6 N/m^2 and 3×10^6 N/m^2 between the metal mold and PMMA substrate during the process. From the figure, different channel depths can be fabricated under different pressures.

4.2. Different channel widths, same pressure and temperature.

PMMA substrates were embossed at 120°C under same pressure with different channel width (1500μm, 1000μm, and 300μm). The comparison of modeled results and experimental data is plotted in Figure 9. From the numerical results, we estimated the pressures to be 18×10^6 N/m^2 between the metal mold and PMMA substrates during the process. From the figure, different channel widths can be fabricated having approximately the same depth.

4.3. Different channel widths, same pressure, different temperature.

PMMA substrates were embossed at 150°C under same pressure with different channel width (1500μm, 1000μm, and 300μm). The comparison of numerical results and experimental data is plotted in Figure 10. Comparing with Figure 9 and Figure 10, there are not many differences between the profiles because Young's modulus varies in a small range when PMMA is above its glass transition temperature. The pressure in this case in 18×10^6 as before.

From Figure 8, Figure 9 and Figure 10, the results indicate a reasonable match between the numerical model of contact-stress analysis and experimental data.

5. CONCLUSION

Hot-embossing process is a flexible and low-cost microfabrication method for building high aspect ratio polymer based microchannels. However, because of the limitation of the physical properties of PMMA, it is difficult to fabricate a sharp straight wall profile for hot-embossed microchannels on PMMA. To quantify the effect of deformation of the wall profile after the hot-embossing process, we found that *contact-stress* analysis is a very good approach to model it. In this paper, we have shown that the *contact-stress* analysis for strain displacement can be used to estimate the wall profile of hot-embossed PMMA microchannels. Comparison with numerical modeling and experiments by varying channel widths, pressures and temperatures were preformed. These results will offer MEMS engineers a tool to predict and design microchannels based on the geometry of micro molds.

REFERENCES:

[1] R. Linnemann, P. Woias, C. D. Senfft, and J. A. Ditterich, "A Self-Priming and Bubble-Tolerant Piezoelectric Silicon Micropump for Liquids and Gases", *IEEE MEMS 1998*, pp. 532-537, 1998.

[2] G. B. Lee, S. H. Chen, G. R. Huang, W. C. Sung, and Y. H. Lin, "Microfabricated Plastic Chips by Hot Embossing Methods and their Applications for DNA Separation and Detection", *Sensors and Actuators* B 75, pp.142-148, 2001.

[3] A. Olsson, O. Larsson, J. Holm, L. Lundbladh, O. Ohman, and G. Stemme, "Valve-less Diffuser Micropumps Fabricated using Thermoplastic Replication", *IEEE MEMS 1997*, pp. 305-310, 1997.

[4] Victor K. W. Li Chong, Kin Fong Lei, Wen J. Li, and Thomas Lee, "Development of Mass-Manufacturable Micro/Nano Fluidic Devices Using Standard CD Fabricatin Technology", *The 1st International Meeting On Microsensors and Microsystems (2003)*, January 12-14, 2003.

[5] Kin Fong Lei, Wen J. Li, Nasser Budraa, and John D. Mai, "Microwave Bonding of Polymer-Based Substrates for Micro/Nano Fluidic Applications", to be published in *The 12th International Conference on Solid-State Sensors, Actuators, and Microsystems (Transducers 03')*, June 8-12, 2003.

[6] John Brydson, *Plastics Materials*, pp. 43-75, Butterworth Heinemann, 1999.

[7] Richard G. Budynas, *Advanced Strength and applied Stress Analysis*, pp.358-361, McGraw-Hill, 1999.

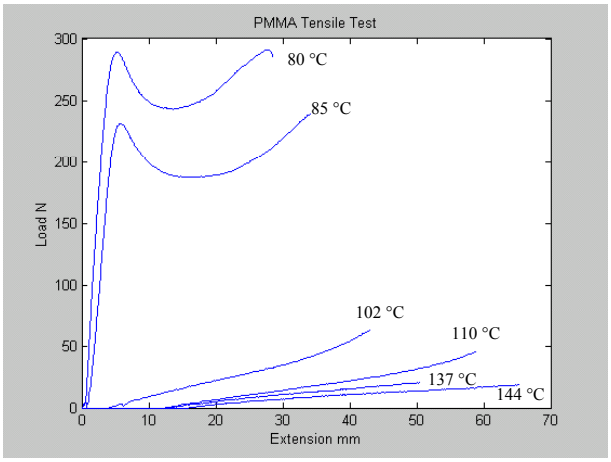

Figure 1. PMMA tensile test result (Load vs. Extension) under different temperature conditions.

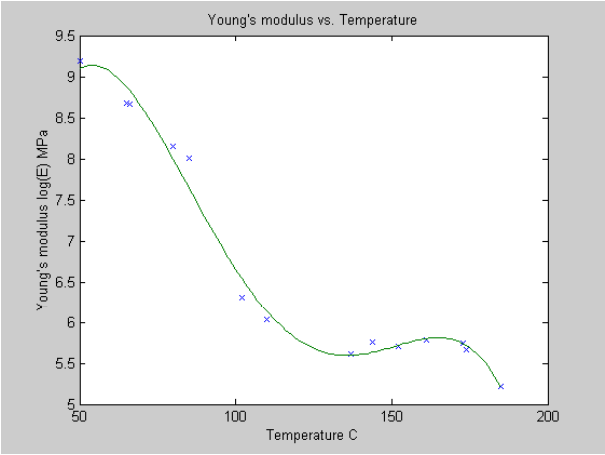

Figure 2. Experimental relationship between Young's modulus and temperature of PMMA samples.

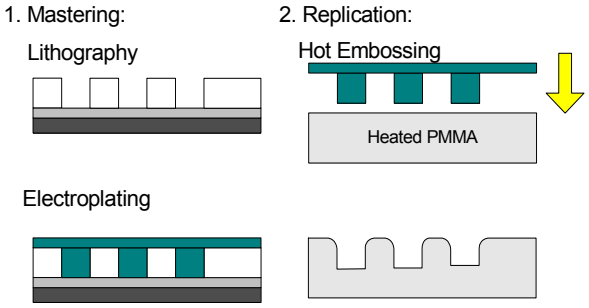

Figure 3. Fabrication process of the micro molding technique: Lithography, Electroplating, and Hot Embossing. However, the resulting channels may not have straight walls.

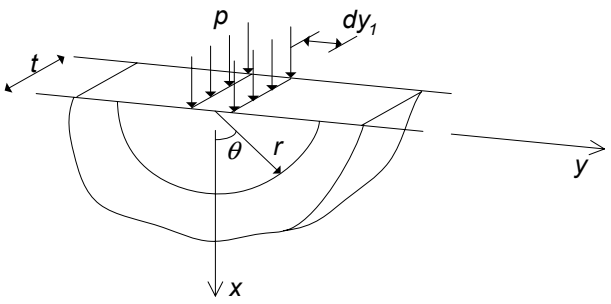

Figure 4. Free body diagram of a contact stress *p* acting on origin.

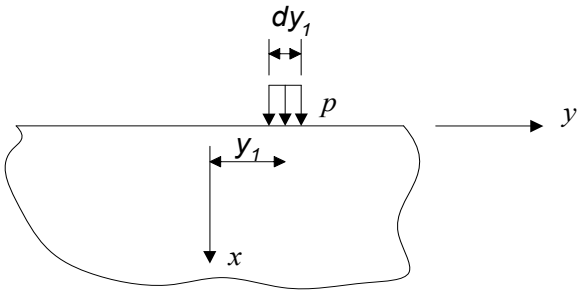

Figure 5. Free body diagram of a contact stress *p* acting on right shifting from the origin.

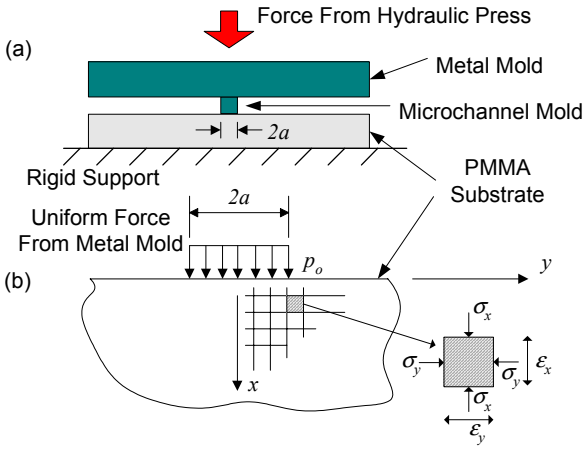

Figure 6. (a) Schematic drawing of hot embossing process using a micro channel mold. (b) Free body diagram of PMMA under a force by a mold and rigid support.

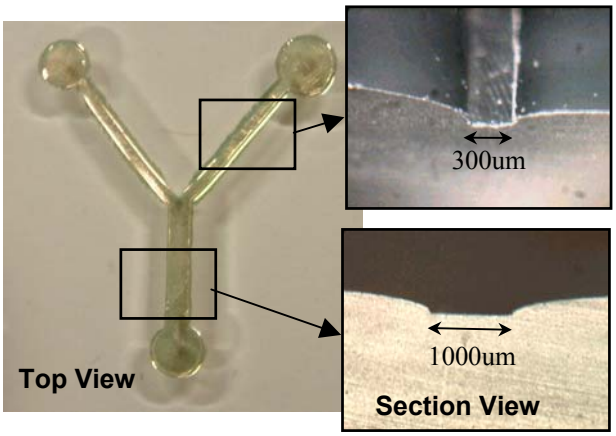

Figure 7. 3D microscope pictures of a PMMA molded with microchannels using hot-embossing process. As shown in the insets on the right, the channel walls are curved due to contact-stress between the mold and PMMA.

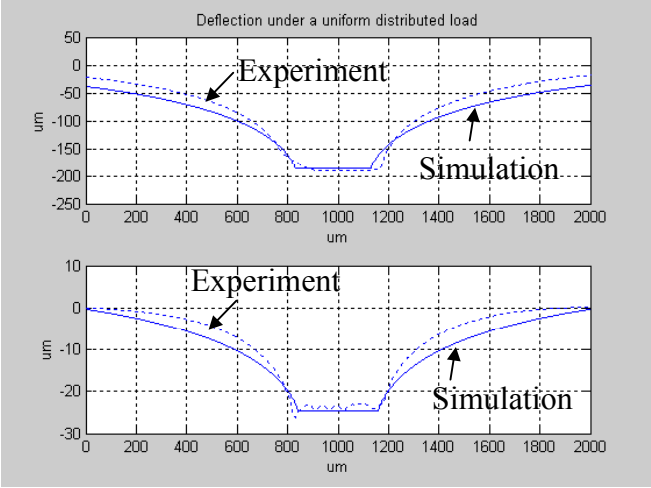

Figure 8. Comparison of modeled (solid line) and experimental (dotted line) channel cross-sectional profile for channels compressed at different pressures with the same width at 120°C.

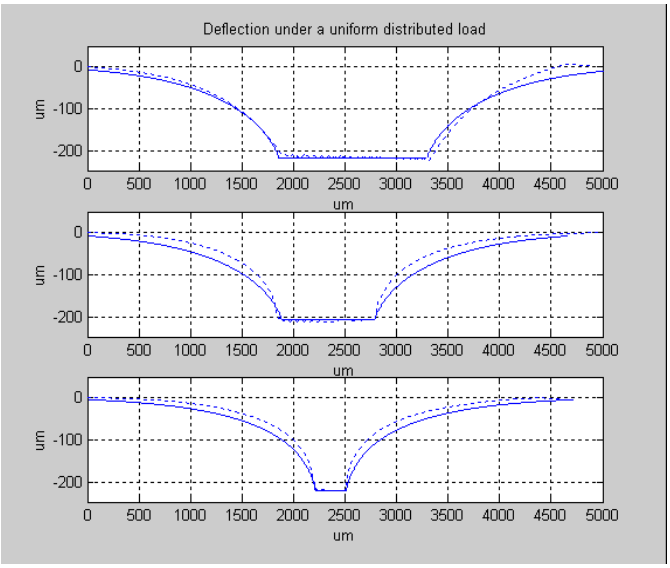

Figure 9. Comparison of modeled (solid line) and experimental (dotted line) channel cross-sectional profile for channels compressed at different channel widths under same pressure at 120°C.

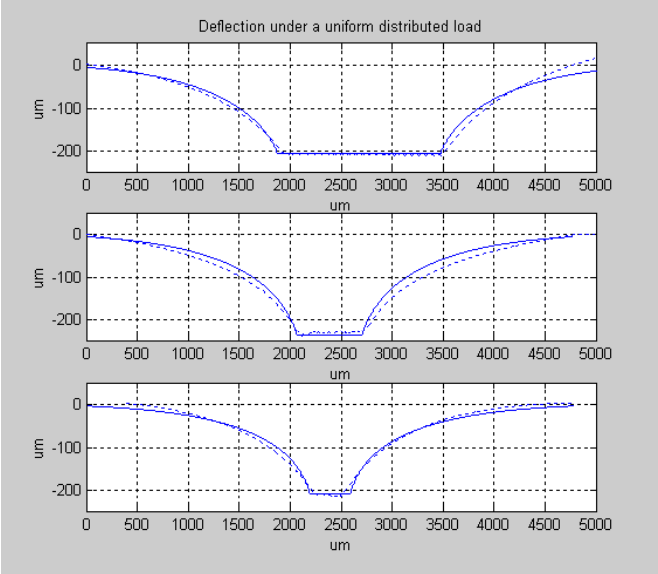

Figure 10. Comparison of modeled (solid line) and experimental (dotted line) channel cross-sectional profile for channels compressed at different channel widths under same pressure at 150°C.